Journal of Engineering Science and Technology Review 17 (2) (2024) 1 - 8

Research Article

JOURNAL OF
Engineering Science and Technology Review

www.jestr.org

Influence Analysis of Contacts on Stress Distributions between Shiplock Structures and Soils

Chao Xu[1,*], Yijia Dong[2] and Liang Ye[1]

[1]*School of Civil Engineering and Architecture, Zhejiang University of Science and Technology, Hangzhou 310000, China*
[2]*College of Water Conservancy and Hydropower Engineering, Hohai University, Nanjing 210000, China*

Received 13 December 2023; Accepted 27 February 2024

Abstract

Hydraulic structures, such as shiplocks, are typically surrounded by backfills, leading to various contact interactions between the backfills and the outer surfaces of the structures. To investigate the evolution of contacts under different loading conditions across the entire structure and to explore the influences of contacts on stress distributions between the shiplock structure and soil, three-dimensional numerical analysis was conducted on the lock head of a shiplock, considering various loading scenarios and contact interactions. Results show that, the opening areas and displacements on the contact surfaces vary significantly during different phases of the construction and operation of the hydraulic structure. The entire process can typically be divided into pouring, backfilling, and water-filling phases, with the backfilling phase showing the largest opening displacement. Compared to calculations without considering the contact, the relative peak maximum principal stress can increase by up to 18.85% when the contact is taken into account, and its peak value is reached after the backfilling process being completed. The conclusions obtained in this study can offer the theoretical and practical references for the design of hydraulic structures and the assessment of their safety.

Keywords: Shiplock; Finite element method; Contact; Opening; Stress redistribution

1. Introduction

Contact is a fundamental aspect of structural systems [1]. Friction and compression at the contact surfaces influence the deformation and stress of the entire system. This is especially important for the hydraulic structures, such as shiplocks, which involve a significant amount of soil-structure contact due to the surrounding backfilled soil. The friction and sliding between the soil and structure have a significant impact on the distribution and magnitude of the stress on the surface of the structure. Changes in the relative positions of soil and structure can lead to the redistribution of stress throughout the entire structural body. Therefore, to accurately understand the influence of contact on structural safety in hydraulic structure design, it is essential to thoroughly investigate variations in the contact status between typical hydraulic structures and soil in three-dimensional space under different loading scenarios, as well as their impact on structural stress. It is crucial to accurately assess the safety of hydraulic structures.

In previous research, most studies on soil-structure interaction have focused on engineering systems, such as retaining wall structures [2-4]. Hydraulic structures, such as shiplocks, especially their lock heads, present inherent complexity for both experimental and simulation studies due to the complex spatial configurations, extensive soil-structure contact areas, and nonlinear characteristics of the subsoil. To simplify the spatial complexity, the three-dimensional structures have been simplified to two-dimensional representations for the numerical analysis of specific lock head types [5, 6]. However, these studies have not considered the impact of structural spatial effects and cannot fully depict the stress distribution on the sidewalls. To better capture stress, three-dimensional lock head models have been developed and used to analyze predefined load combinations [7]. Nevertheless, these studies were unable to effectively account for the impact of the backfilling process and could not fully capture the evolution of the contact state.

In order to fully comprehend the three-dimensional contact behavior of a lock head, considering the impact of the backfilling process and its effect on the magnitude and distribution of structural stress, a finite element contact analysis was conducted on a typical lock head structure. A detailed comparison was made with an analysis that did not consider contact. Given that shiplocks were typically built on soft soil foundations, the Duncan-Chang model was utilized to simulate the soil, aiming to achieve a more accurate representation of the structural system's response.

2. State of the art

Numerous numerical methods have been proposed in previous studies for accurately solving contact problems. The finite element model (FEM) for conducting research on the contact phenomena was previously developed [8] and has continued to evolve up to the present [9]. Furthermore, various emerging methods for facilitating contact analysis have been proposed, such as the particle finite element method [10], smoothed particle hydrodynamics method [11], discrete element method [12], and material point-finite element coupling method [13]. However, the FEM remains the most popular approach for analyzing complex contact problems owing to significant advancements in commercial software. Therefore, the FEM was adopted in this study. Additionally, several types of contact problems have been investigated, including frictionless contact [14], large

*E-mail address: xuchao@zust.edu.cn
ISSN: 1791-2377
doi:10.25103/jestr.172.01

deformation contact [15], discontinuous contact [16], and other engineering contact problems [17-19]. Among various contact problems, the soil-structure contact problem between the soil and the deformed structure is essential for this study, and this problem has attracted significant attention from numerous scholars [20, 21]. However, the aforementioned studies have not paid attention to evolution state and influence of contact on stress distributions between the shiplock structure and soil, especially for structures like the shiplock.

The shiplock serves as a crucial infrastructure on channels and rivers, facilitating navigation. Water transportation significantly benefits from its pivotal role. As a conventional hydraulic structure, the lock head of a shiplock is a complex and sophisticated construction [22]. Meanwhile, this structure involves various characteristics, such as extensive excavation and deep burial [23], resulting in substantial contact areas between the outer surfaces of concrete structures and backfills. The status of contact demonstrates variations when subjected to different loading conditions. In this context, significant effort has been exerted to enhance the accuracy of structural analysis through extensive research [24, 25]. Gao et al. [26, 27] conducted investigations on contact-related issues in gates and lock chambers. They utilized the finite element method as their primary approach to investigate nonlinear contacts. In practical lock projects, a variety of contact elements are frequently used, including non-thickness elements [5] and Desai elements [6]. These elements have the potential to offer considerably accurate and detailed understanding of the internal forces within projects implemented using emerging technologies. These studies always focused on a specific case that could not demonstrate evolutions of contact state under different loading conditions. Furthermore, the studies that aim to quantitatively analyze influencing factors (e.g., friction forces on wall backs), which may have been disregarded in past research, have been conducted; the findings offer valuable insights into the redistribution of stress within the lock head under different contact conditions [7, 28]. However, contact behaviors under backfilling loads have not received much attention.

Reviewing the literature indicates that the majority of research in this particular field has been on investigating two dimensional scenarios. However, the lock head is a sophisticated structure encompassing water corridors and hollow spaces, and there is a scarcity of studies that have explored the complete structure in three-dimensional coordinates. Given that the lock head structure frequently exhibits notable spatial effects, conducting rudimentary two-dimensional analyses may lead to an underestimation of the influences of structural complexities. Therefore, a comprehensive three-dimensional model should be used to enhance analyses of the shiplock, taking into account contact.

To investigate the evolutions of contact state between the lock head structure and surrounding soils under various load cases and the influences of contacts on structural stresses, the finite element model of a full lock head-foundation-backfills system in the three-dimensional space was developed and corresponding analysis was conducted. The researchers used the Duncan-Chang model [29, 30] to effectively simulate the nonlinearity of the soil foundation. The analysis involves contacts between the floor and foundation, as well as the interactions between walls and backfills.

The rest of this study is organized as follows. Section 3 provides a brief summary of the constitutive models adopted to describe soils and contacts. This section also presents and analyzes an engineering construction project. Section 4 explores the changes in contact status and evaluates the impact of different opening statuses on structural stresses, and finally, the conclusions are summarized in Section 5.

3. Methodology

3.1 Duncan-Chang model

The Duncan model is a widely used nonlinear model in engineering applications and is invaluable for simulating elastic soils. Its applicability extends across a series of scenarios, offering a significant representation of soil deformation with a balance between accuracy and computational complexity, particularly when compared with more complicated soil models. To determine the stress–strain responses of soil, Kondner [31] conducted an extensive series of triaxial tests and proposed the following hyperbolic expression:

$$\sigma_1 - \sigma_3 = \frac{\varepsilon_a}{a + b\varepsilon_a} \tag{1}$$

where, a and b are constants; ε_a represents the maximum principal strain; σ_1 is the maximum principal stress in the stress space, and σ_3 corresponds to the minimum principal stress.

The original model was modified on the basis of the established hyperbolic expression, particularly by developing an incremental elastic model called the Duncan-Chang model. In the early version of this model, the Poisson's ratio was always supposed to be an unchanged value for calculations [29]. Thereafter, this assumption was modified and two variations of the Duncan-Chang model were proposed: (1) the *E-v* model, in which the Poisson's ratio is related to stress [32]; and (2) the *E-B* model, in which the bulk modulus is related to stress [33]. The present study utilizes the *E-v* model in all simulations. The physical interpretations of the parameters in this model are as follows.

3.1.1 Tangent elastic modulus E_t

Based on the hyperbolic relation, Mohr-Coulomb law, and the linear correlation between $\log(E_i/p_a)$ and $\log(\sigma_3/p_a)$, the tangent elastic modulus expressed in Eq. (2) was developed by Duncan and Chang [30].

$$E_t = Kp_a\left(\frac{\sigma_3}{p_a}\right)^n \left(1 - R_f S\right)^2 \tag{2}$$

$$S = \frac{\left(1-\sin\varphi\right)\left(\sigma_1 - \sigma_3\right)}{2c\cos\varphi + 2\sigma_3\sin\varphi} \tag{3}$$

where, S is called the stress level and K and n are constants derived from experimental tests. The parameter c represents the cohesion force of the tested soils, which is one of the two soil parameters derived from a series of tested Mohr's circles. The second parameter, denoted as φ, refers to the internal friction angle. The term R_f signifies the failure ratio, conventionally constrained to values below 1.0 [30]. In addition, p_a corresponds to atmospheric pressure, incorporated to neutralize the influences of the unit system. E_i is the initial tangent elastic modulus, which is typically

determined by the initial tangent slope derived from the (σ_1-σ_3)-ε_a curve. It is noteworthy that the tangent elastic modulus is synonymous with the reciprocal of parameter a as depicted in Fig. 1.

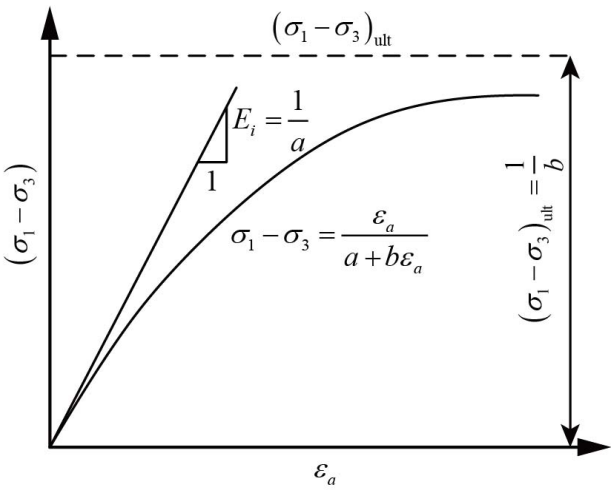

Fig. 1. Diagram of the (σ_1-σ_3) - ε_a curve from a triaxial test.

3.1.2 Tangent poisson's ratio v_t

Kulhawy et al. [32] showed that the correlation between the axial strain ε_a and the negative value of the lateral expansion strain-ε_r can be fitted with a hyperbolic curve. The tangent slope of the curve is called tangent Poisson's ratio, and the value of this parameter can be calculated using the following equations:

$$v_t=\frac{1}{(1-A)^2}\left[G-F\log\left(\frac{\sigma_3}{p_a}\right)\right] \tag{4}$$

where, F and G are test constants, and A is defined in the following form:

$$A=\frac{D(\sigma_1-\sigma_3)}{Kp_a\left(\frac{\sigma_3}{p_a}\right)^n\left[1-\frac{R_f}{2}\frac{(1-\sin\varphi)(\sigma_1-\sigma_3)}{\sigma_3\sin\varphi+c\cos\varphi}\right]} \tag{5}$$

where, D is a test constant.

The value of Poisson's ratio may be larger than 0.5 owing to soil dilatancy. However, adopting a Poisson's ratio exceeding 0.5 during finite element analyses can result in a singular coefficient matrix. Therefore, if the Poisson's ratio exceeds 0.49, then it is constrained to 0.49.

3.1.3 Unloading-reloading elastic modulus E_{ur}

The Duncan-Chang model utilizes the unloading-reloading elastic modulus to distinguish recoverable and unrecoverable parts of the deformation. The modulus can be mathematically expressed as follows:

$$E_{ur}=K_{ur}p_a\left(\frac{\sigma_3}{p_a}\right)^n \tag{6}$$

where, K_{ur} is a test constant and n is the same as the one used in Eq. (2).

3.2 Implementation of Duncan-Chang model

In the present study, numerical calculations of the contact problem are conducted using the finite element method. This method discretizes the domain containing soil and concrete structures into discrete elements. Apart from the contact areas, each element has a strong connection with other elements that share nodes with it. External loads are distributed among these nodes. Moreover, the finite element method has been widely employed for solving various governing equations and obtaining displacements, strains, and stresses.

Finite element analysis was conducted by using the ABAQUS software in this study. To incorporate the Duncan-Chang model, a user material subroutine (UMAT) was created in FORTRAN to compute appropriate stiffness matrices. The primary function of UMAT is to calculate stress increments and final stress at the end of the current increment step, based on the strain increments provided by ABAQUS. Thereafter, UMAT updates the defined state variables. Moreover, it must provide the Jacobian matrix, and the matrix element ($[J]_{ij}$) represents the partial derivative of the i^{th} element of the incremental strain vector with respect to the j^{th} element of the incremental stress vector. The Jacobian matrix can be used for controlling the convergence rate of the nonlinear iteration process.

Within the development of UMAT, the midpoint method was utilized to compute the incremental value of the stress and final stress state of the Duncan-Chang model during the current increment step. The computational procedure is depicted in Fig. 2. The process was divided into five major parts: input step, three updating steps (as indicated by 1, 2, and 3 in Fig. 2), and output step. The input information primarily includes the stress state and strain increments obtained from the previous increment step, calculation parameters of the Duncan-Chang model, and defined state variables. For the Duncan-Chang model, the defined state variables include deviatoric stress (σ_1-σ_3) and stress level (as defined in Eq. (3)). Within the updating steps, parameters E_t and v_t must be calculated for forming the stiffness matrix. Before calculating these values, a necessary step is needed to determine the deviatoric stress and stress level based on the current stress state. Thereafter, a comparison was made with the historical maximum values of deviatoric stress and stress level. If both current values are lower than the historical maximum values, then the unloading-reloading elastic modulus is used. The stress state used in the first updating step is the initial stress at the beginning of the current increment step. The second updating step uses the average of the results from the first step and initial stress. The third updating step utilizes the results obtained from the second updating step.

3.3 Contact model

The lock head of the ship lock is a complex structure characterized by extensive excavation, deep burial, and considerable volume of concrete. Given the significant differences in material properties, slippage or even cracking may occur at contact surfaces between concrete and soil. Contact between concrete and soil can be divided into two main categories [34].

3.3.1 Normal pressure

Contact problem in construction is typically regarded as a hard contact. When two bodies come into contact and are compressed, they generate normal pressure. This pressure disappears when contact surfaces separate, as illustrated in

Fig. 3. Normal stress and relative displacement can be described as follows [5]:

$$\begin{cases} \sigma_a = 0, \quad \sigma_n = 0, \quad \Delta u_n \geq 0 & \text{Open} \\ \sigma_n \geq 0, \quad \Delta u_n = 0 & \text{Contact} \end{cases} \tag{7}$$

where, u represents the displacement, σ_n is the normal part of the stress, σ_a is the tangent part, and Δ denotes the increment.

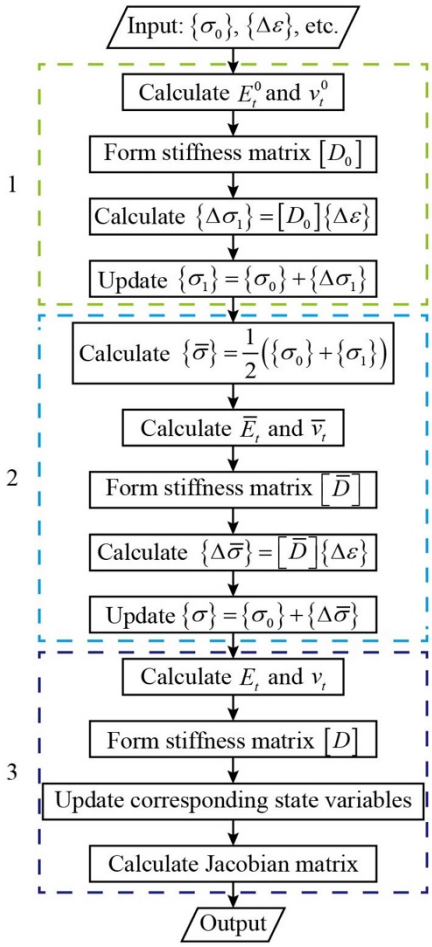

Fig. 2. Flowchart of the computational procedure in UMAT.

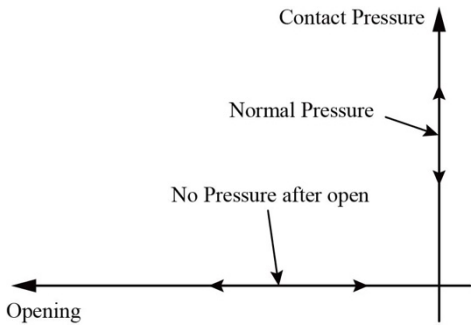

Fig. 3. Interdependence diagram of contact pressure and opening in hard contacts

3.3.2 Friction force

Friction arises between two contact surfaces when these surfaces come into contact and resist motion resulting from other forces. Friction load can be obtained using the Mohr-Coulomb friction formula as follows:

$$\tau_f = \mu p \tag{8}$$

where, p represents the normal pressure originating from the interaction between contact surfaces and μ is the friction coefficient. If external forces exceed the friction force, then the contact surfaces start sliding. Otherwise, they remain bonded.

The correlation between tangent stress and tangent displacement can be described as follows [5]:

$$\begin{cases} \sigma_a \leq \mu\sigma_n, \Delta du_a = 0 & \text{Bonding} \\ \sigma_a = \mu\sigma_n, \Delta du_a \geq 0 & \text{Sliding} \end{cases} \tag{9}$$

3.4 Project background

The lock head of the studied ship lock has a horizontal length of 28.5 m along the river and width of 53.8 m across the river. The height ranges from -6.5 m to 5.4 m. This lock head is symmetric along the Y-Z plane, so only half of the geometry in the river-crossing direction is simulated. The entire geometry of the lock head-foundation-backfills system has been meshed, as presented in Fig. 4.

The lock head is a massive concrete structure cast in layers. It can be seen consisting of three main sections: floor, water corridor, and hollow space sections. Backfill materials are layered during construction. The construction sequence is illustrated in Fig. 5.

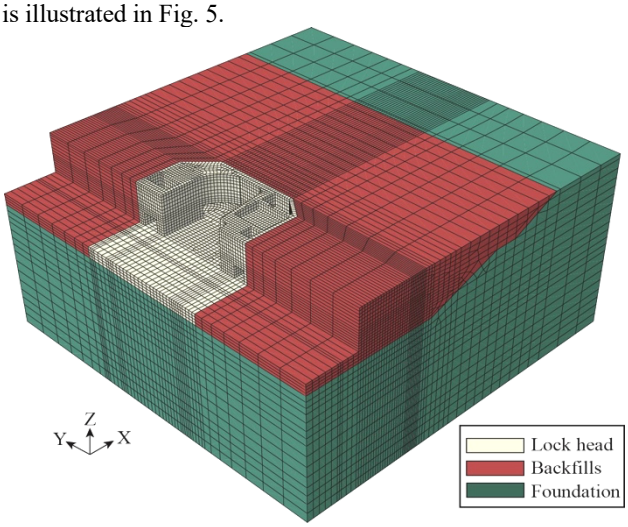

Fig. 4. Finite element mesh for numerical analyses of the lock head.

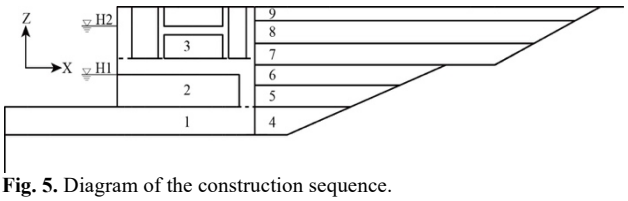

Fig. 5. Diagram of the construction sequence.

3.5 Material properties

To simplify the calculation, all materials in the analysis are assumed to be isotropic. Elastic modulus and bulk density of concrete are set to 30 GPa and 24.5 kN/m^3, respectively. The value of 0.167 is adopted for the Poisson's ratio of concrete.

The subsoil beneath the lock head structure comprises four soil layers with different soil properties. The material properties of all layers are described using the *E-v* model, with the calculation parameters listed in Table 1 [6, 35, 36].

Table 1. Calculation parameters in the *E-v* model of the foundation

Layer	γ (kN/m^3)	K	n	R_f	φ (°)	c (kPa)	G	F	D	K_{ur}
1	17.7	500	0.37	0.6	26	10	0.14	0.1	0	1000
2	17.9	350	0.37	0.7	19	11	0.14	0.1	0	700
3	18.8	350	0.37	0.6	30	10	0.14	0.1	0	700
4	18.7	350	0.37	0.6	23	10	0.14	0.1	0	700

Contact conditions have been specified between the top face of the first soil layer beneath the lock head structure (designated as the slave surface) and the bottom face of the concrete floor (designated as the master surface). Contacts are defined between the backfills (designated as the slave surface) and external surfaces of the walls (designated as the master surface). These contact interactions are modeled as hard contacts, using the Mohr–Coulomb friction model to characterize tangential contact, with the friction coefficient set to 0.35 [37-39].

4. Results Analysis and Discussion

The analysis covers three load cases: pouring, backfilling, and water-filling cases. The water-filling case encompasses two scenarios: water filled to the top of corridors (H1 in Fig. 5) and water filled to the maximum navigable stage of the channel (H2 in Fig. 5).

4.1 Evolutions of the contact status

During the pouring phase of concrete, contacts primarily occur at the surfaces between the floor and foundation. The analysis results indicate that these contacts are fully closed during this phase. As backfills are filled, contact surfaces begin to open gradually, as illustrated in Fig. 6.

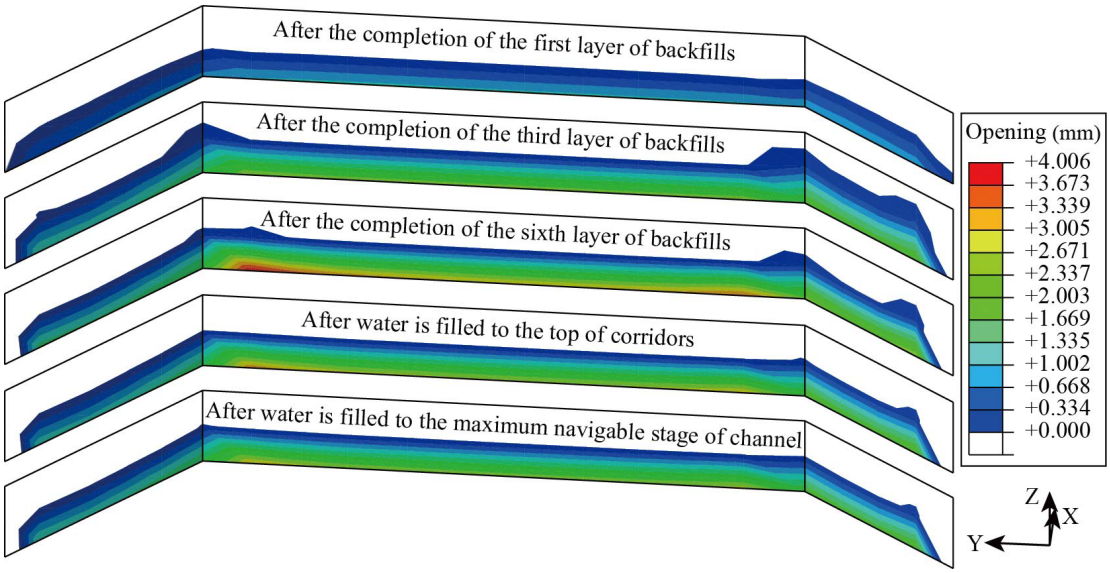

Fig. 6. Opening of contact surfaces between lateral walls across the river and backfills.

Initially, contact opening occurs in the bottom layer of backfilled soils, and the opened area is concentrated in the chamfer and lateral walls. As the height of backfills increases, the opening area gradually expands, but changes are relatively small. Meanwhile, the maximum opening displacement changes sharply and reaches 1.1 mm when the first layer of backfills is completed. The opening displacement reaches 4.0 mm when all backfills are completed. In addition, there is a reduction in the opening area as the lock head fills with water, and the opening displacement decreases as water level rises. The reason for this phenomenon is that the load generated by water pressure causes the opening area to close.

Fig. 7 illustrates that the most prevalent contact openings occur on the outer surface of the walls along the river. Furthermore, the calculation results indicate that these openings are mainly located on the middle part of the floor and top of the backfills. The opening displacements of contact surfaces between the middle part of the floor and backfills are small, and they are inversely proportional to the filled height of backfills. By contrast, the opening displacements are positively proportional to the filled height of backfills at the contact surfaces between the top part of the backfills and the walls.

Contact areas between the top face of the first soil layer beneath the lock head structure and the bottom face of the floor are initially closed when backfills begin to fill. Fig. 8 shows that until the fourth layer of backfills is completed, the openings begin to occur with the maximum opening displacement reaching 1.375 mm. As the backfills fill, the opening area gradually expands. After the completion of all backfills, the maximum opening displacement increases to 10.41 mm.

After the shiplock is completed, the water level in the lock head will rise during operations. Figs. 6 to 8 demonstrate that after water-filling, the opening area shrinks and displacements of contact surfaces reduce caused by the effects of water pressure. Fig. 6 indicates that contacts between walls in the river-crossing direction and backfills remain nearly unchanged. However, Fig. 7 reveals that the opening area of contact surfaces between the middle part of the floor and backfills increases, while it decreases significantly on the contact surfaces between walls and the top part of backfills. In the case of contact surfaces between

the floor and foundation, Fig. 8 demonstrates that openings almost disappear after the water level reaches the maximum navigable stage of the channel.

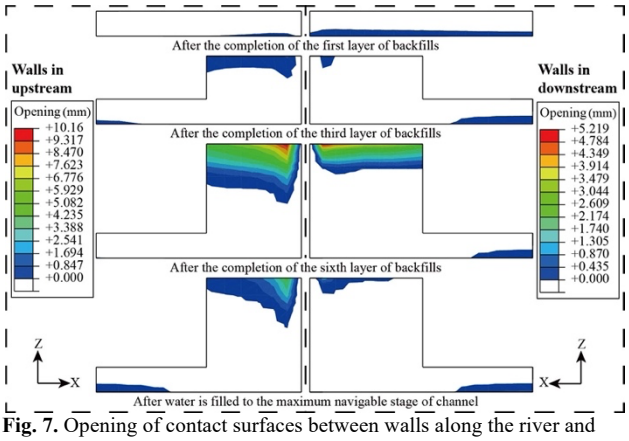

Fig. 7. Opening of contact surfaces between walls along the river and backfills.

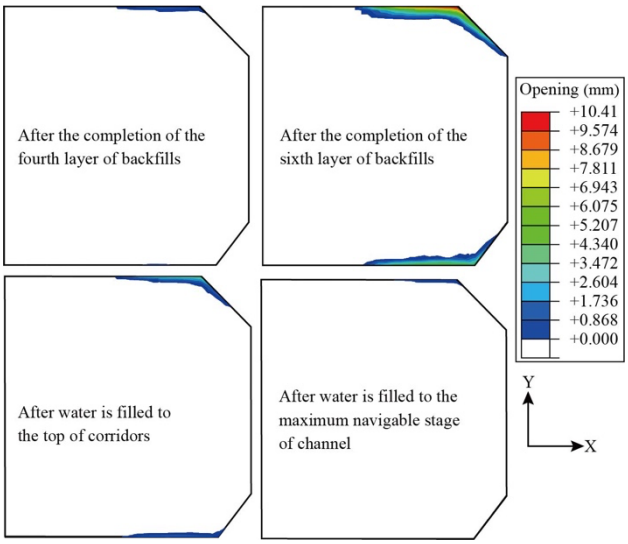

Fig. 8. Opening of contact surfaces between the floor and the foundation.

4.2 Influences of contacts on structural stresses

Constraints on the outer surfaces of the lock head change with the varying contact statuses. When contact surfaces are closed, the structure is constrained on these surfaces by contact forces. Conversely, when the contact surfaces open, the surfaces become free. Therefore, changes in contact statuses will cause redistributions of structural stresses, which affect the lock head performance.

To explore the impact of contacts on structural stresses, calculations were carried out with and without contact effects. The obtained results in Table 2 indicate that contacts have a substantial influence on the peak value of the maximum principal stress (σ_{max}). The absolute value of the relative increment is up to 18.85% when the water is filled to the maximum navigable stage of the channel. In general, the peak value calculated without considering contacts is relatively lower during the construction phase but significantly higher when the shiplock is in operation.

The analysis of the calculation results demonstrates that contacts have a significant impact on stress distributions. Fig. 9 shows the differences in maximum principal stress distributions for scenarios with and without consideration of contacts. The calculations without contact interactions overestimate the stress development of the structure. As shown in Fig. 8, the maximum opening displacement can be observed at the intersections of chamfers and walls. This location is where stress distribution is apparently different between cases with and without consideration of contacts, as shown in Fig. 9. Three specific sections along the river (Y-axis) are depicted in Fig. 10. Evidently, the middle section (Y= -0.5 m), which is farthest from the chamfer, experiences the smallest change in the maximum principal stress distribution.

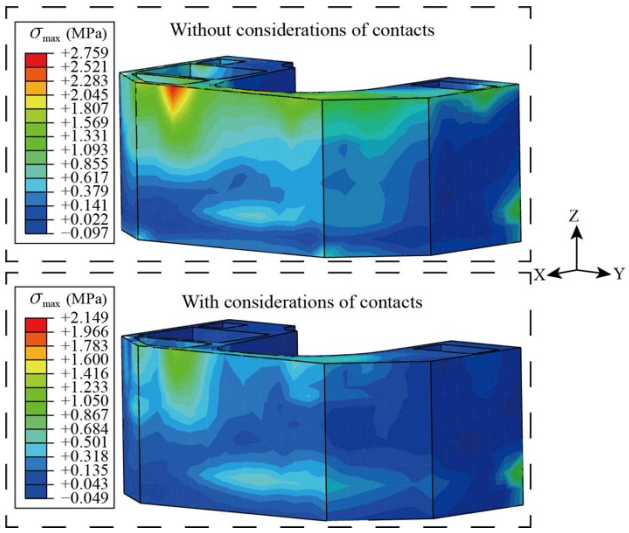

Fig. 9. Distributions of σ_{max} on the outer surfaces of walls after the completion of backfills

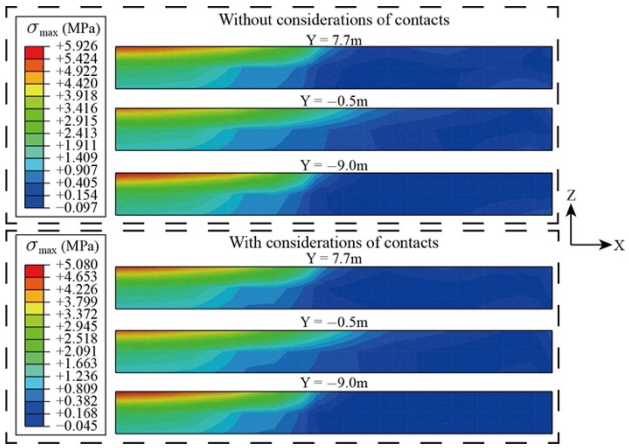

Fig. 10. Distributions of σ_{max} at sections extracted from the floor along Y-axis

Table 2. Peak values of σ_{max} in the lock head at six time points (MPa)

Name	TP1	TP2	TP3	TP4	TP5	TP6
Without contact	1.18	0.88	2.76	6.44	5.40	3.94
With contact	1.33	0.91	2.77	5.48	4.64	3.20
Difference/MPa	0.15	0.02	0.01	-0.96	-0.76	-0.74
%	12.81	2.72	0.25	-14.90	-14.08	-18.85

Note: TP1 is the time after pouring of concrete; TP2 is the time after completion of the first layer of backfills; TP3 is the timeafter completion of the third layer of backfills; TP4 is the time after completion of the sixth layer of backfills; TP5 is the time after water is filled to the top of corridors; TP6 is the time after water is filled to the maximum navigable stage of channel.

5. Conclusions

The primary emphasis of the current investigation centers on the lock head of a shiplock, chosen as a representative hydraulic structure. The comprehensive analysis extends to the entire superstructure-foundation-backfill system. Within this analytical framework, the nonlinear elastic behavior of the subsoil and backfilled soil was described by the Duncan-Chang model. In addition, an appropriate contact model was used at all contact surfaces, effectively determining the complex interactions between concrete structures and soil. The main conclusions can be obtained as following:

(1) Contacts significantly affect structural stresses and their distribution on contact surfaces. Contacts were found to increase the relative peak maximum principal stress by up to 18.85%. This result demonstrates the importance of considering contacts during feasibility studies and design phases.

(2) The evolution of contact statuses can be divided into three periods: before backfilling, after backfilling, and after operating. Contacts are closed before backfilling and gradually open after backfilling, with the opening area and displacements increasing. When the ship lock is operating and water is filled, the opening area and displacements decrease.

(3) When backfilling begins, contact openings appear. Opening surfaces exist mainly at the bottom and top layers of backfills. The opening area and opening displacements reach the maximum value after the completion of backfilling. The evolution of contact status and a variety of stress results provide guidance for similar hydraulic structures.

This study focuses on a specific lock head type, resulting in qualitative research findings that can serve as references for similar projects. For other projects, quantitative analysis is necessary to obtain accurate results. In addition, soil essentially exhibits elasto-plastic behavior. Therefore, a more sophisticated constitutive model should be adopted to describe the soil more precisely, instead of the Duncan-Chang model, which is only capable of determining nonlinear elasticity.

Acknowledgements

The authors are grateful for the support provided by the Science Project of Zhejiang Institute of Hydraulics & Estuary, China (FZJZSYS21006).

References

[1] N. Kikuchi and J. T. Oden, *Contact Problems in Elasticity: A Study of Variational Inequalities and Finite Element Methods*. Philadelphia, PA, USA: SIAM, 1988.

[2] Javadi, R. Hassanli, M. M. Rahman, and M. R. Karim, "Self-centring segmental retaining walls-A new construction system for retaining walls," *Front. Struct. Civ. Eng.*, vol. 15, no. 4, pp. 980-1000, Aug. 2021.

[3] N. Psarropoulos, Y. Tsompanakis, and M. Katsirakis, "Dynamic soil-structure interaction between retaining walls, retaining soil and retained structures," *Earthq. Eng.*, vol. 20, no. 7, pp. 3593-3617, May 2022.

[4] C. Yoo and K. M. Lee, "Instrumentation of anchored segmental retaining wall," *Geotech. Test. J.*, vol. 26, no. 4, pp. 382-389, Dec. 2003.

[5] Z. Cao, J. Lian, and X. Liu, "The influence of friction between wall back and soil on the stress in ship-lock floors and its improvement measures," *J. Hydroelectr. Eng. (China)*, vol. 33, no. 2, pp. 208-213, Apr. 2014.

[6] Q. Zhou, L. Bian, and Z. Xu, "A study on algorithm for lock head floor of shiplock of separately casted floor and piers," *Port Waterw. Eng. (China)*, no. 1, pp. 43-46, Jan. 2003.

[7] L. Wang and B. Yang, "Analysis of nonlinear finite element for internal force of navigation lock head," *Port Eng. Technol. (China)*, vol. 48, no. 6, pp. 28-31, Dec. 2011.

[8] L. R. Herrmann, "Finite element analysis of contact problems," *J. Eng. Mech. Div.*, vol. 104, no. 5, pp. 1043-1057, Oct. 1978.

[9] F. Massa, H. Do, O. Cazier, T. Tison, and B. Lallemand, "Finite element analysis of frictionless contact problems using fuzzy control approach," *Eng. Comput.*, vol. 32, no. 3, pp. 585-606, May 2015.

[10] J. M. Carbonell, L. Monforte, M. O. Ciantia, M. Arroyo, and A. Gens, "Geotechnical particle finite element method for modeling of soil-structure interaction under large deformation conditions," *J. Rock Mech. Geotech. Eng.*, vol. 14, no. 3, pp. 967-983, Jun. 2022.

[11] J. Wang and D. Chan, "Frictional contact algorithms in SPH for the simulation of soil-structure interaction," *Int. J. Numer. Anal. Methods Geomech.*, vol. 38, no. 7, pp. 747-770, May 2014.

[12] S. Li and A. Smith, "Relationship between acoustic emission and energy dissipation: a DEM study of soil–structure interaction," *Acta Geotech.*, vol. 18, no. 6, pp. 2971-2990, Jun. 2023.

[13] Z. Lei, B. Wu, S. Wu, Y. Nie, S. Cheng, and C. Zhang, "A material point-finite element (MPM-FEM) model for simulating three-dimensional soil-structure interactions with the hybrid contact method," *Comput. Geotech.*, vol. 152, Dec. 2022, Art. no. 105009.

[14] F. Sewerin and P. Papadopoulos, "On the finite element solution of frictionless contact problems using an exact penalty approach," *Comput. Methods Appl. Mech. Eng.*, vol. 368, Aug. 2020, Art. no. 113108.

[15] V. Agrawal and S. S. Gautam, "Varying-order NURBS discretization: An accurate and efficient method for isogeometric analysis of large deformation contact problems," *Comput. Methods Appl. Mech. Eng.*, vol. 367, Aug. 2020, Art. no. 113125.

[16] İ. Çömez, M. A. Güler, and S. El-Borgi, "Continuous and discontinuous contact problems of a homogeneous piezoelectric layer pressed by a conducting rigid flat punch," *Acta Mech.*, vol. 231, no. 3, pp. 957-976, Mar. 2020.

[17] A. A. Churkin, A. Yu. Khmel'nitskii, and V. V. Kapustin, "Evaluation of soil-structure contact state by normalized acoustic response analysis," *Soil Mech. Found. Eng.*, vol. 59, no. 5, pp. 453-458, Nov. 2022.

[18] M. Yaylacı, M. Abanoz, E. U. Yaylacı, H. Ölmez, D. M. Sekban, and A. Birinci, "Evaluation of the contact problem of functionally graded layer resting on rigid foundation pressed via rigid punch by analytical and numerical (FEM and MLP) methods," *Arch. Appl. Mech.*, vol. 92, no. 6, pp. 1953-1971, Jun. 2022.

[19] X. Ma, H. Lei, and X. Kang, "Examination of interface roughness and particle morphology on granular soil-structure shearing behavior using DEM and 3D printing," *Eng. Struct.*, vol. 290, Sept. 2023, Art. no. 116365.

[20] X. Liu, A. Zhou, S. L. Shen, J. Li, and A. Arulrajah, "Modelling unsaturated soil-structure interfacial behavior by using DEM," *Comput. Geotech.*, vol. 137, Sep. 2021, Art. no. 104305.

[21] X. Yang, Z. Xu, J. Chai, Y. Qin, and J. Cao, "Numerical investigation of the seepage mechanism and characteristics of soil-structure interface by CFD-DEM coupling method," *Comput. Geotech.*, vol. 159, Jul. 2023, Art. no. 105430.

[22] C. Su and J. Bai, "Structural optimization of ship lock heads during construction period considering concrete creep," *Math. Probl. Eng.*, vol. 2020, Aug. 2020, Art. no. e5495202.

[23] R. Kauther, H. Montenegro, and O. Stelzer, "Back analysis of geotechnical models for a deep excavation in claystone based on monitoring data," in *Proc. XVI Eur. Conf. Soil Mech. Geotech. Eng.*, Edinburgh, UK, Sept. 2015, pp. 607-612.

[24] Z. Qian, Z. Ma, S. Jiang, C. Du, F. Zhang, and J. Liu, "Finite element model of sheet-pile structures with underground retaining walls in Gaogang second-line shiplock project and its numerical verification," *Adv. Sci. Technol. Water Resour. (China)*, vol. 35, no. 6, pp. 62-67, Nov. 2015.

[25] C. Xu, C. Su, and F. Sheng, "Contact analysis and foundation reinforcement measures of ship lock on soft foundation," in *Proc. 10th Int. Conf. Anal. Discontinuous Deformation*, Honolulu, USA, Dec. 2011, pp. 413-418.

[26] Z. Gao, Y. Hu, and H. Wang, "Nonlinear contact finite element analysis on bottom pintle of sector gate," *J. Water Resour. Water Eng. (China)*, vol. 28, no. 1, pp. 174-179, Feb. 2017.

[27] N. Zhang, Y. Guan, F. Li, and W. Xia, "Monitoring and analysis of stress and deformation on unloading lock under backfill load," *Yellow River (China)*, vol. 41, no. 5, pp. 138-142, May 2019.

[28] Q. Lu, X. Liu, J. Yang, Z. Zhou, and Y. Fan, "Simulation and analysis of the stress influence of lock gatefloor by different construction process," *J. Transp. Sci. Eng. (China)*, no. 1, pp. 48-52, Mar. 2003.

[29] J. M. Duncan and G. W. Clough, "Finite element analyses of port allen lock," *J. Soil Mech. Found. Div.*, vol. 97, no. 8, pp. 1053-1068, Aug. 1971.

[30] J. M. Duncan and C. Y. Chang, "Nonlinear analysis of stress and strain in soils," *J. Soil Mech. Found. Div.*, vol. 96, no. 5, pp. 1629-1653, Sept. 1970.

[31] R. L. Kondner, "Hyperbolic stress-strain response: cohesive soils," *J. Soil Mech. Found. Div.*, vol. 89, no. 1, pp. 115-143, Feb. 1963.

[32] F. H. Kulhaway, J. M. Duncan, and H. B. Seed, "Finite element analyses of stresses and movements in embankments during construction," University of California, Berkeley, California, USA, Tech. Rep. CR-S-69-8, Nov. 1969.

[33] J. M. Duncan, P. Byrne, K. S. Wong, and P. Mabry, "Strength, stress-strain and bulk modulus parameters for finite element analysis of stresses and movements in soil mass," University of California, Berkeley, California, USA, Tech. Rep. UCB/GT/80-01, Aug. 1980.

[34] K. Fei and J. Zhang, *Application of ABAQUS in Geotechnical Engineering.* Beijing, China: Posts & Telecom Press, 2017.

[35] S. R. Wang, C. L. Li, Z. W. Liu, and J. B. Fang, "Optimization of construction scheme and supporting technology for HJS soft rock tunnel," *In. J. Min. Sci. Technol.*, vol. 24, no. 6, pp. 847-852, Dec. 2014.

[36] B. Qin, D. H. Rui, S. R. Wang, M. C. Ji, and Z. S. Zou, "Experimental investigation on formation and evolution characteristics of frozen wall under salty groundwater seepage," *J. Eng. Sci. Technol. Rev.*, vol. 13, no. 6, pp. 99-107, Dec. 2020.

[37] X. Chang, B. F. Gu, S. R. Wang, and S. Y. Wang, "Behavior of laterally loaded cast-in-Place (CIP) piles with double steel casings embedded in bare hard rock in deep water areas." *Comput. Geotech.*, vol. 160, May 2023, Art. no. 105513.

[38] L. Cheng, X. Chang, S. R. Wang, Y. F. Wang, and M. X. Zhang, "Effect analysis of bedding plane and fracture distribution on crack propagation process in layered fractured rock mass," *J. Eng. Sci. Technol. Rev.*, vol. 14, no. 5, pp. 90-99, Nov. 2021.

[39] X. Chang, J. Q. Sun, S. R. Wang, A. Z. Kang, and J. C. Peng, "Horizontally loaded steel pipe piles anchored in bare and hard rock under deep water condition: Parametric analysis," *Ocean Eng*., vol. 266, Sept. 2022, Art. no. 112715.